RASĀYAN *J. Chem.*
Vol. 18 | No. 2 |1130-1137| April - June | 2025
ISSN: 0974-1496 | e-ISSN: 0976-0083 | CODEN: RJCABP
http://www.rasayanjournal.com
http://www.rasayanjournal.co.in

COMPARATIVE STUDY OF PHOTOCATALYTIC DEGRADATION OF INDIGO CARMINE DYE USING NICKEL DOPED AND UNDOPED NANO COBALT (II) OXIDE AS PHOTOCATALYST

N. Singh✉, M. Jangid, R. Vyas and R. Ameta
Department of Chemistry, PAHER University, Udaipur-313003 (Rajasthan), India
✉Corresponding author: nirmalsingh0068@gmail.com

ABSTRACT

Advanced oxidation processes (AOPs) have been used as an alternative and effective option for the treatment of industrial wastewater, especially in the case of non-biodegradable compounds. In the present work, the photocatalytic degradation of Indigo carmine (IC) has been studied under visible light in the presence of nanocrystalline Nickel-doped Cobalt (II) oxide as a photocatalyst. Undoped cobalt (II) oxide and Nickel-cobalt (II) oxide were synthesized by using the Sol-gel method. These synthesized photocatalyst was characterized by using techniques such as Field Emission Scanning Electron Microscopy (FESEM), Energy Dispersive X-ray spectroscopy (EDX), X-ray Diffraction (XRD), Fourier Transform Infrared spectroscopy (FTIR), and High Resolution Transmission Electron Microscopy (HRTEM). The effect of various parameters like pH, concentration of dye, amount of photocatalyst, light intensity, etc., on the rate of photocatalytic degradation of the dye was studied. It was observed that at optimum experimental parameters, 78.57% of dye was degraded by Nickel-doped Cobalt oxide, while only 55.27% of dye was degraded in the case of undoped cobalt oxide in 180 min. of contact time with the photocatalyst.

Keywords: Indigo carmine, Nanocrystalline, Nickel-doped Cobalt (II) oxide, Undoped Cobalt (II) oxide, photocatalyst, photocatalytic degradation.

RASĀYAN *J. Chem.*, Vol. 18, No. 2, 2025

INTRODUCTION

In recent years, novel methods have gained a lot of attention in adsorption methodologies, from textile industries to the treatment of wastewater.[1] Advanced oxidation processes (AOPs) have been used as an alternative and effective option and broadly applied for the treatment of different types of industrial wastewater, especially in the case of non-biodegradable compounds.[2] Various researchers synthesized or fabricated cobalt oxide and its composites for the degradation of different types of organic or inorganic pollutants like phenol,[3] methyl violet, methylthionine chloride,[4] rhodamine B, direct red 80.[5] Semiconductors like ZnO,[6-8] TiO_2 and its other composites[9-12] were used as photocatalyst for the treatment of textile dyes in wastewater. Alansi *et al.,*[13] fabricated BiOBr nanoparticles loaded on reduced graphene oxide for photocatalytic degradation of Rhodamine-B and observed 100% photodegradation activity of G-BiOBr as compared to BiOBr under visible light irradiation. Synthesis of cobalt vanadate nanostructures for photocatalytic degradation of organic dyes was carried out by Ghiyasiyan-Arani *et al.*[14] Gemeay *et al.,*[15] investigated the kinetics of the oxidative degradation of the indigo carmine with hydrogen peroxide catalyzed with the supported five metal complexes. They observed that the reactivity of catalysts is dependent on the redox potential of the metal ions, the amount of complex loaded per gram of dry catalyst, the type of ligand, and the support. Moreover, the reaction rate was strongly dependent on the pH of the medium, the cationic and anionic surfactants, and the irradiation with UV light. Influence of physicochemical–electronic properties of transition metal ion doped polycrystalline titania on the photocatalytic degradation of Indigo Carmine and 4-nitrophenol under UV/solar light was carried out by Devi and Kumar.[16] Agorku *et al.,*[17] prepared C, N, S-doped ZrO_2 and Eu-doped C, N, S-ZrO_2 photocatalysts and observed the photocatalytic activity towards Indigo carmine. The highest photocatalytic activity towards Indigo carmine was observed for the Eu, C, N, S-doped ZrO_2 (0.6 mol.% Eu) sample, and the commercial ZrO_2 showed the lowest photodegradation activity. They concluded that the control of Eu doping in the C, N, S-ZrO_2 was very important in reducing electron-hole recombination.

http://doi.org/10.31788/RJC.2025.1826118

EXPERIMENTAL

Materials and Methods

Cobalt (II) chloride (Hexahydrate), Nickel chloride (Hexahydrate), Sodium carbonate (Anhydrous) was used in the present study. These are of analytical grade and used without further purification. Indigo Carmine was purchased from Himedia chemicals. All the solutions were prepared in double distilled water (DDW).

General Procedure

Synthesis of composite: Synthesis of composite was done in two steps; firstly, synthesis of Cobalt oxide and then followed by doping of synthesised Cobalt oxide.

Step 1: Synthesis of CoO

In the first step, the solution of Cobalt chloride and Sodium carbonate was taken in separate beakers and then mixed with continuous stirring until the formation of purple color gel. Thereafter it was washed with doubly distilled water (DDW) and filtered. The gel was then dried in an oven for 24 hours by which black color cobalt oxide was obtained. Purple color change into black color due to the removal of CO_2.

Step 2: Doping of Nickel on CoO

For Ni doping on CoO, a solution of Nickel chloride and CoO was taken. This reaction was completed with magnetic stirring for 30 minutes and washed with DDW and it was dried in an oven in 100°C for 4 hours. After this, a black color mixture was obtained.

Detection Method

Photodegradation Study

A stock solution of Indigo carmine (1.0×10^{-3} M) was prepared by dissolving 0.0466 g of dye in 100 mL. Double-distilled water. This stock solution was further diluted. The absorbance of Indigo carmine solution was determined with the help of a spectrophotometer (Systronics Model 106) at λ_{max} = 608 nm. The photocatalytic degradation of Indigo carmine dye was studied after the addition of 0.10 g of the composite Ni-CoO in 50 mL dye solution (4.8×10^{-5} M). The reaction mixture was exposed to visible light with a 200 W tungsten lamp. Absorbance of the solution was measured with the help of a spectrophotometer (Systronics Model 106) at several time intervals. The intensity of light was varied by changing the distance between the light source and the reaction mixture. A digital pH meter (Systronics Model CL-54) was used to measure the pH of the solution. pH of the dye solution was adjusted by the addition of previously standardized 0.1 N sulfuric acid and 0.1 N sodium hydroxide solutions. Control experiments were carried out to confirm that the degradation of Indigo carmine was photocatalytic.

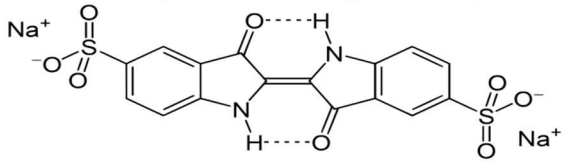

Fig.-1: Structure of Indigo carmine ($C_{16}H_8N_2Na_2O_8S_2$)

A graph was plotted between log A v/s time, which was a straight line showing that photocatalytic degradation of IC follows pseudo-first order kinetics. The rate constant for the degradation of dye was calculated by the following equation:

$$k = 2.303 \times \text{slope} \quad (1)$$

RESULTS AND DISCUSSION

Characterization

Field Emission Scanning Electron Microscopy (FESEM)

To study the morphology of the as-synthesized doped and undoped composite, the Field Emission Scanning Electron Microscopy (FESEM) analysis technique was used. Obtained images of undoped and Ni-doped CoO are given below (Fig.-2 A-D). From the obtained images, it was found that Ni was successfully doped and Ni-CoO was obtained in a spherical shape.

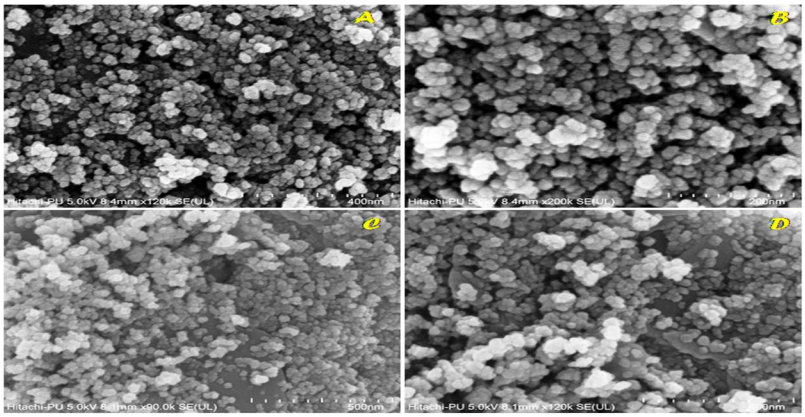

Fig.-2: FESEM of Undoped CoO (A, B) and Ni-doped CoO (C, D)

Energy-Dispersive X-Ray Spectroscopy (EDX) Analysis

Energy-dispersive X-ray spectroscopy (EDX) data revealed that only Nickel, Cobalt, and Oxygen are present, without any impurities. The results are reported in (Fig.-3).

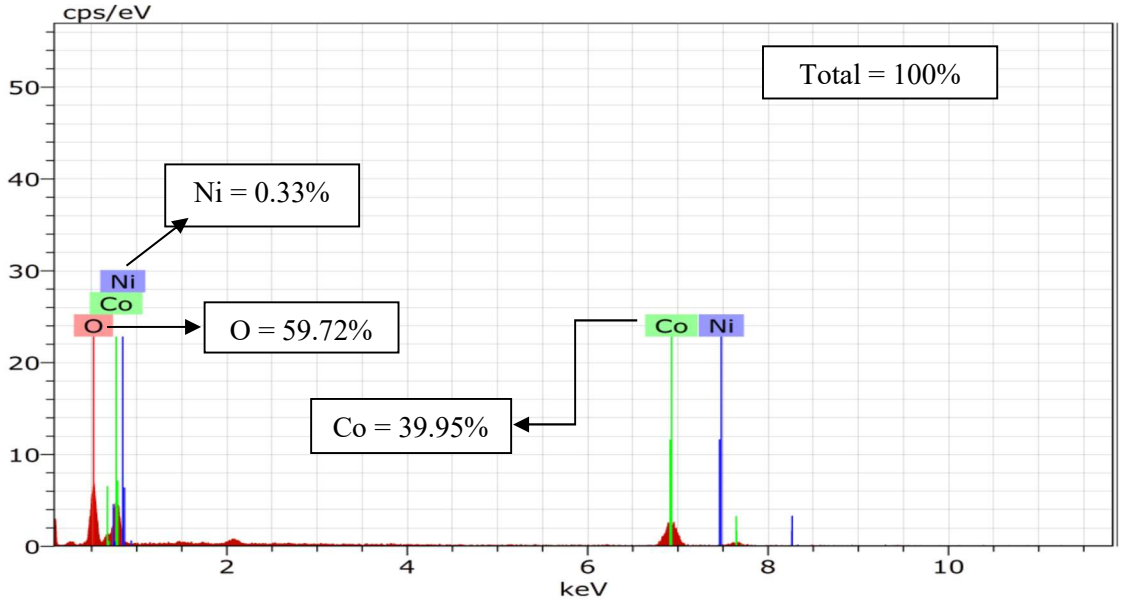

Fig.-3: EDX of Ni-doped CoO

X-ray Diffraction (XRD)

The X-ray pattern of the nanocomposite (Ni-CoO) is shown in Fig.-4). The average particle size for the composite (Ni-doped CoO) was calculated using the Debye-Scherrer equation, and it was found to be 13-25 nm, which was also confirmed by HRTEM.

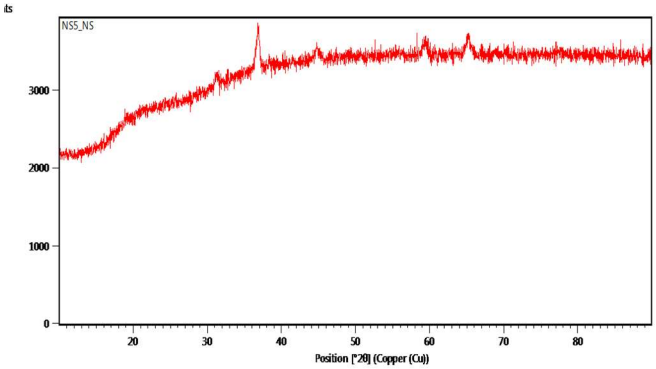

Fig.-4: XRD of Ni-doped CoO

Fourier-Transform Infrared (FTIR)

FTIR spectrum was recorded using an FT-Infra-Red spectrophotometer model RZX (Perkin-Elmer) to determine the different functional groups present in the composite (Ni-CoO). In case of the composite (Ni-CoO), a broad peak at 3430.3 cm^{-1} represents O-H stretching vibrations of the C-OH groups and water molecule. The IR spectra show a strong band at 1631 and 1556 $cm^{-1,}$ which corresponds to the carboxylate ion. The peak around 662 cm^{-1} corresponds to the bending modes of vibration of cobalt oxide, and that around 569 cm^{-1} corresponds to bending modes of vibration of nickel oxide present in the composite.[18]

High-Resolution Transmission Electron Microscopy (HRTEM)

HRTEM images were taken to determine the shape and size of nanocrystalline Ni-CoO. It is seen that the nanocrystals are less cubic and the particle size was in the range of 13-25 nm (Fig.-5). It is clear that no agglomeration of nanoparticles takes place, and morphology seems to be indexed on the cubic, spinel structure of the nanoparticles. HRTEM recorded on the Tecnai G2 20 (FEI) S-Twin 200 kV transmission electron microscope.

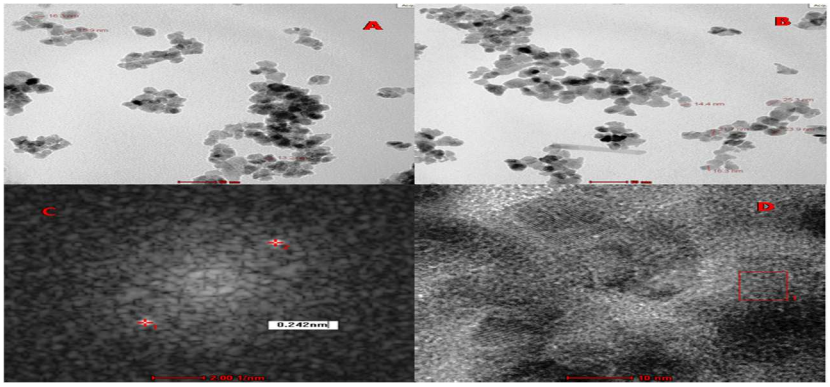

Fig.-5: HRTEM (A, B), and Diffractogram (C, D) of composite

Typical Run

A typical run has been drawn for the photocatalytic degradation of IC using the photocatalyst Ni-CoO. Where all the parameters were kept constant (Table-1 and Fig.-6).

Table-1: pH = 7.5, [Indigo carmine] = 4.8 x 10^{-5} M, Composite = 0.10 g, Light intensity = 60.0 mW cm^{-2}

Time (min)	Ni-CoO		CoO	
	Absorbance (A)	1 + log A	Absorbance (A)	1 + log A
0	0.728	0.8621	0.720	0.8573
30	0.531	0.7251	0.623	0.7945
60	0.456	0.6590	0.527	0.7218
90	0.342	0.5340	0.462	0.6646
120	0.267	0.4265	0.418	0.6212
150	0.210	0.3222	0.347	0.5403
180	0.156	0.1931	0.322	0.5079

[Rate constant (k) Ni-CoO= 14.39 x 10^{-5} s^{-1}] [Rate constant (k) CoO= 7.33 x 10^{-5} s^{-1}]

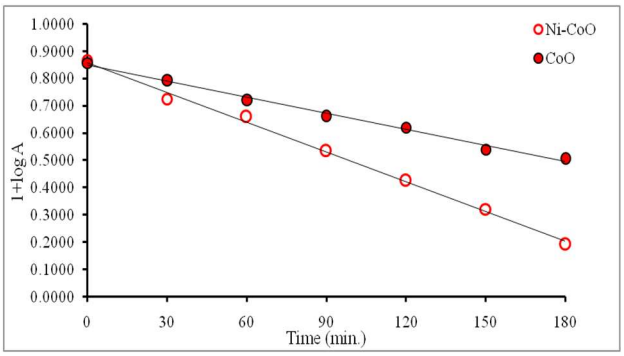

Fig.-6: Typical Runs

Effect of pH

The effect of variation of pH was studied in the range 5.5-9.0. The results are graphically represented in (Fig.-7). It was observed that the rate increases with an increase in pH up to 7.5, but the rate of degradation decreases with a further increase in pH. An electron from the conduction band is abstracted by dissolved oxygen to generate $O_2^{\bullet -}$. An increase in the rate of photocatalytic degradation of Ni-CoO with the increase in pH may be due to the availability of more $O_2^{\bullet -}$ anion radicals. A decrease in the rate of photocatalytic degradation of the Ni-CoO may be because Ni-CoO is present in its anionic form, which will experience a force of repulsion with the negatively charged surface of the composite due to adsorption of more OH^- ions on the surface of the composite. The composite was found to be active in the almost neutral range. [Indigo carmine] = 4.8 x 10^{-5} M, Composite = 0.10 g, Light intensity = 60.0 mW cm^{-2}].

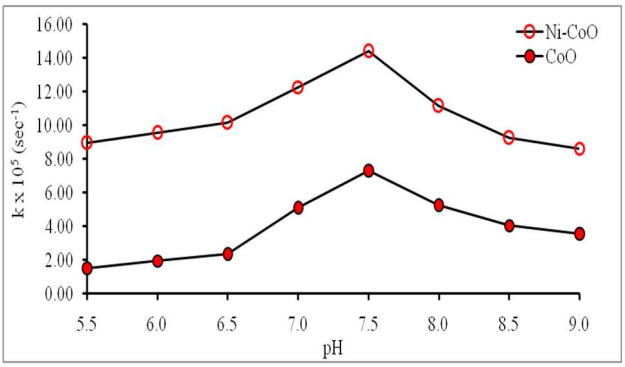

Fig.-7: Variation of Rate Constant with pH

Effect of Dye Concentration

The effect of dye concentration on the photocatalytic degradation of Indigo carmine was observed in the range of 4.0 x 10^{-5} to 5.4 x 10^{-5} M, and the results are graphically presented in (Fig.-8). As the concentration of the dye was increased, it was observed that the dye degradation increased, because more dye molecules are available for excitation and energy transfer, but after 4.8 x 10^{-5} M, the photocatalytic degradation showed a declining behavior. This may be because at higher concentrations of dye, dye molecules start acting as a filter for the incident light, and they do not allow the desired light intensity to reach the composite particles and thus resulting in a decrease in the rate of the photocatalytic degradation of dye. [pH = 7.5, Composite = 0.10 g, Light intensity = 60.0 mW cm^{-2}].

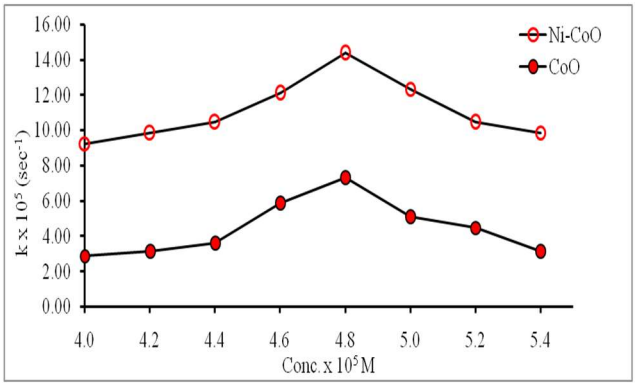

Fig.-8: Variation of Rate Constant with Concentration

Effect of the Amount of Semiconductor

The effect of variation of the amount of composite on the rate of dye degradation has been studied in the range from 0.02 to 0.14 g. The results of the variation of the rate constant with the photocatalyst are represented in Fig.-9). It was observed that as the amount of photocatalyst was increased, the rate of photocatalytic degradation increased. The rate of degradation was found to be maximum at 0.10 g of the semiconductor, because the exposed surface area was also increased, but after a certain limit, when the amount of semiconductor was increased further; there was no increase in the exposed surface area of the photocatalyst, but multilayers are formed making e^- - h^+ recombination more probable. Thus, a decrease in

the rate of degradation was observed. [pH = 7.5, [Indigo carmine] = 1.2 x 10^{-5} M, Light intensity = 60.0 mW cm^{-2}].

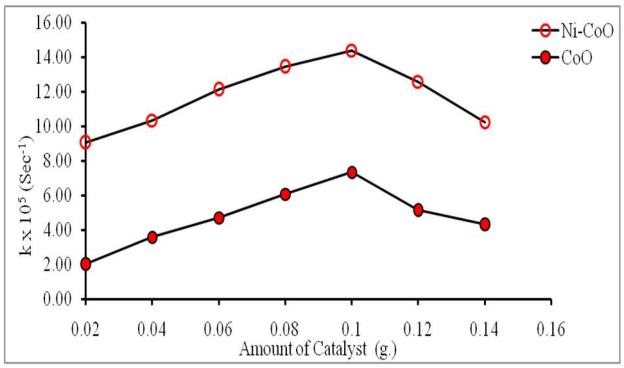

Fig.-9: Variation of Rate Constant with Amount of Photocatalyst

Effect of Light Intensity

The effect of the light intensity on the photocatalytic degradation of Indigo carmine was studied by varying the light intensity from 20.0 to 70.0 mW cm^{-2}. Rate constants with different light intensities are represented in (Fig.-10. It was observed that the rate of photocatalytic degradation of Indigo carmine was found to be increased with an increase in the intensity of light, as the number of photons striking per unit area of photocatalyst surface per unit time will also increase. The maximum rate was observed at 60.0 mW cm^{-2} for the degradation of Indigo carmine. However, at higher light intensities, some thermal side reactions may also start, and hence, the rate of photocatalytic degradation was slightly decreased on increasing the intensity of light further. [pH = 7.5, [Indigo carmine] = 1.2 x 10^{-5} M, Composite = 0.10 g].

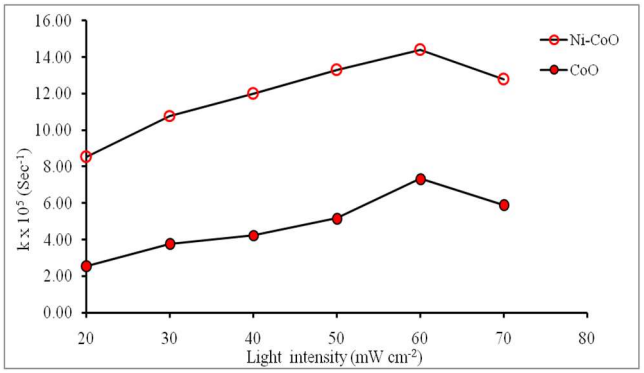

Fig.-10: Variation of Rate Constant with Light Intensity

Mechanism

The mechanism for the photocatalytic degradation of Indigo carmine (IC) using Ni-CoO photocatalysts has been proposed. Electrons in Ni-CoO are excited to its conduction band on light irradiation. •OH radicals were not found as an active oxidizing species, and this was confirmed by using a hydroxyl radical scavenger (2-propanol), where the rate of degradation was not affected appreciably. Based on the observations, a tentative mechanism for the photocatalytic degradation of Indigo carmine has been proposed as:

$$^1IC_0 \xrightarrow{h\upsilon} {}^1IC_1$$

$$^1IC_1 \xrightarrow{ISC} {}^3IC_1$$

$$CoO \xrightarrow{h\upsilon} CoO\ (h^+\ (VB) + e^-\ (CB))$$

$$O_2\ (\text{Dissolved Oxygen}) + e^-\ (CB) \longrightarrow O_2^{\bullet -}$$

In basic medium:

$$^3IC_1 + O_2^{\bullet -} \longrightarrow \text{Leuco IC}$$

$$\text{Leuco IC} \longrightarrow \text{Products}$$

Indigo carmine absorbs radiation of suitable wavelength, and it is excited to its first excited singlet state, followed by intersystem crossing (ISC) to the triplet state. On the other hand, the photocatalyst Ni-CoO also utilizes the incident light energy to excite its electrons from the valence band to the conduction band,

thus leaving behind a hole. The dissolved oxygen accepts the electron from the conduction band and converts to superoxide radical ion, which transforms the Indigo carmine into its leuco form. The leuco form is ultimately unstable, and it will degrade into smaller products.

CONCLUSION

The nanocrystalline Ni-CoO composites have been prepared successfully by the sol-gel method. The nanostructure of composite samples was characterized by FESEM, EDX, XRD, FTIR, and HRTEM. The experimental results show that the degradation efficiency of Indigo carmine was affected by various working parameters like pH (7.5), concentration (1.2 x 10^{-5} M), Dose of composite (0.10 g), and light intensity (60.0 mW cm-2). Photocatalytic treatment is likely to increase the quality of polluted water. The observation of the present work will provide new avenues for the possible use of Ni-doped other photocatalysts for better photocatalytic performance.

ACKNOWLEDGEMENTS

Authors are thankful to Prof. S.C. Ameta, Department of Chemistry, PAHER University, Udaipur for their help in the course of this work and to SAIF, CIL, Chandigarh for FESEM, EDS and XRD & IIT Delhi for HRTEM analysis of samples.

CONFLICT OF INTERESTS

The authors declare that there is no conflict of interest.

AUTHOR CONTRIBUTIONS

All the authors contributed significantly to this manuscript, participated in reviewing/editing and approved the final draft for publication. The research profile of the authors can be verified from their ORCID ids, given below:

Nirmal Singh http://orchid.org/0009-0008-7866-8955
Monika Jangid http://orchid.org/0000-0002-3630-7974
Ritu Vyas http://orchid.org/0009-0003-1778-9124
Rameshwar Ameta http://orchid.org/0009-0001-2218-6075

REFERENCES

1. V. Kavithayeni, K. Geetha, and S. Akash Prabhu, *International Journal of Recent Technology and Engineering*, **7**, 332(2019).
2. Y. Deng and R. Zhao, *Current Pollution Reports*, **1(3)**, 167(2015), https://doi.org/10.1007/s40726-015-0015-z
3. J. Bai, *Materials Letters*, **63(17)**, 1485(2009), https://doi.org/10.1016/j.matlet.2009.03.052
4. F. Xia, E. Ou, L. Wang and J. Wang, *Dyes and Pigments*, **76(1)**, 76(2008), https://doi.org/10.1016/j.dyepig.2006.08.008
5. C. R. Dhas, R. Venkatesh, K. Jothivenkatachalam, A. Nithya, B. S. Benjamin, A. M. E. Raj, et al., *Ceramics International*, **41(8)**, 9301(2015), https://doi.org/10.1016/j.ceramint.2015.03.238
6. S. Chakrabarti, and B. K. Dutta, *Journal of hazardous materials*, **112(3)**, 269(2004), https://doi.org/10.1016/j.jhazmat.2004.05.013
7. C. Vidya, M. C. Prabha, and M. A. Raj, *Environmental Nanotechnology, Monitoring & Management*, **6**, 134(2016), https://doi.org/10.1016/j.enmm.2016.09.004
8. P. Franco, O. Sacco, I. De Marco, and V. Vaiano, *Catalysts*, **9(4)**, 346(2019), https://doi.org/10.3390/catal9040346
9. B. Neppolian, H. C. Choi, S. Sakthivel, B. Arabindoo, and V. Murugesan, *Journal of hazardous materials*, **89(2-3)**, 303(2002), https://doi.org/10.1016/S0304-3894(01)00329-6
10. K. Subramani, K. Byrappa, S. Ananda, K. L. Rai, C. Ranganathaiah, and M. Yoshimura, *Bulletin of Materials Science*, **30(1)**, 37(2007), https://doi.org/10.1007/s12034-007-0007-8

11. N. Barka, A. Assabbane, A. Nounah, and Y. A. Ichou, *Journal of hazardous materials*, **152(3)**, 1054(2008), https://doi.org/10.1016/j.jhazmat.2007.07.080
12. L. L. Costa, and A. G. Prado, *Journal of Photochemistry and Photobiology A: Chemistry*, **201(1)**, 45(2009), https://doi.org/10.1016/j.jphotochem.2008.09.014
13. M. Alansi, M. Al-Qunaibit, I. O. Alade, T. F. Qahtan, and T. A. Saleh, *Journal of Molecular Liquids*, **253**, 297(2018), https://doi.org/10.1016/j.molliq.2018.01.034
14. M. Ghiyasiyan-Arani, and M. Masjedi-Arani, *Journal of Molecular Catalysis A: Chemical*, **425**, 31(2016), https://doi.org/10.1016/j.molcata.2016.09.023
15. H. Gemeay, I. A. Mansour, R. G. El-Sharkawy, and A. B. Zaki, *Journal of Molecular Catalysis A: Chemical*, **193(1-2)**, 109(2003), https://doi.org/10.1016/S1381-1169(02)00477-6
16. L. G. Devi, and S. G. Kumar, *Applied Surface Science*, **257(7)**, 2779(2011), https://doi.org/10.1016/j.apsusc.2010.10.062
17. E. S. Agorku, A. T. Kuvarega, B. B. Mamba, A. C. Pandey, and A. K. Mishra, *Journal of Rare Earths*, **33(5)**, 498(2015), https://doi.org/10.1016/S1002-0721(14)60447-6
18. N. J. Tharayil, R. Raveendran, A. V. Vaidyan, and P. G. Chithra, *Indian Journal of Engineering & Materials Sciences*, **15**, 489(2008).

[RJC-6118/2025]